

Monte Carlo simulations of small-angle elastic scattering events

M. Vos and M. Went

Atomic and Molecular Physics Laboratory, Research School of Physical Sciences and Engineering, The Australian National University, Canberra ACT 0200, Australia

(Received 23 August 2005; revised manuscript received 12 October 2005; published 2 December 2005)

Quantitative interpretation of electron spectroscopy is almost always dependent on the understanding of multiple scattering effects. Monte Carlo simulations are often used to model multiple scattering effects, as this method provides for a conceptually simple framework for incorporating both elastic and inelastic scattering processes. In this paper, we demonstrate that when small-angle deflections are important, diffraction effects become significant, and straightforward Monte Carlo simulations are not expected to be valid. However, a simple modification to the Monte Carlo procedure is presented that uses cluster-derived elastic scattering cross sections rather than those derived from isolated atoms. In this way we can incorporate diffraction effects in the simulations. Results from electron momentum spectroscopy are presented to illustrate these effects. These modified simulations greatly improve the agreement between experiment and theory, and this approach builds a bridge between Monte Carlo and diffraction-based interpretations of experiments.

DOI: 10.1103/PhysRevB.72.233101

PACS number(s): 61.14.-x, 79.20.Hx

In electron-spectroscopy and electron-microscopy experiments, knowledge of the transport properties of energetic electrons through matter is of crucial importance for understanding the results. Inelastic processes will reduce the energy of the electrons involved, whereas elastic scattering will change the direction of propagation. For example, the lateral resolution and probing depth in a scanning Auger experiment depends critically on both processes. Understanding these processes has been a major endeavor in applied physics.

One of the main techniques that has proven fruitful in understanding these processes is Monte Carlo (MC) modeling.^{1,2} In these studies the elastic and inelastic scattering processes are treated independently. The inelastic scattering properties are derived from the dielectric functions of the material. Elastic scattering processes are modeled using the differential elastic scattering cross section of *isolated* atoms. This is a semiclassical approach and the electrons are treated as particles with well-defined trajectories. The mean separation of successive elastic and inelastic multiple scattering events is determined by their mean free paths λ_{el} and λ_{inel} , respectively. The elastic mean free path is related to the total (atomic) elastic scattering cross section σ_{el}

$$\lambda_{el} = \frac{1}{N\sigma_{el}}, \quad (1)$$

with N the number of atoms per unit volume.

On the other hand it is known that electrons can diffract. This phenomenon forms the basis of image formation in an electron microscope. For polycrystalline samples (and to a lesser extent for amorphous ones), the angular distribution of the transmitted beam show strong rings that reflect the crystal structure and are not part of the differential cross section of a single atom. For keV electrons, diffraction is observed for small scattering angles, typically $<10^\circ$. Here the intensity of the diffracted beams as a function of depth can be calculated using the dynamical theory of diffraction. This approach depends on the wave nature of electrons.

Most MC simulations of elastic scattering are focused on

transport properties such as the length l of the trajectory of an electron traversing a layer of thickness t . Such properties are not affected severely by small-angle deflections. For large-angle deflections (corresponding to large momentum transfers), the Debye-Waller factor is small and thus, diffraction effects are minor. Recent papers by Smekal *et al.*³ and by Liljequist⁴ compare the results of MC simulations to those of quantum calculations.

One case where small deflections have a huge impact on the outcome of the measurement is electron momentum spectroscopy (EMS). In this technique, a well-collimated electron beam impinges on a thin film, and transfers a large part of its energy to a target electron, which is subsequently ejected from the film. The scattered and ejected electron are subsequently detected in coincidence. In the independent-particle approximation, the binding energy ε and momentum \mathbf{q} of the ejected electron *before* the collision is given by

$$\varepsilon = E_0 - E_1 - E_2, \quad (2)$$

$$\mathbf{q} = \mathbf{k}_1 + \mathbf{k}_2 - \mathbf{k}_0 \quad (3)$$

with $E_{0,1,2}$ the energy of the incoming, scattered and ejected particle, and $\mathbf{k}_{0,1,2}$ the momentum of the incoming, scattered, and ejected electron, respectively. In our experiment, $E_0 = 50$ keV and $E_{1,2} = 25$ keV.

The momentum resolution of these experiments is about 0.1 a.u. [1 atomic unit (a.u.) of momentum corresponds to $\approx 1.89 \text{ \AA}^{-1}$]. This is much less than most reciprocal lattice vectors. Thus diffraction will have a large influence on the outcome of an EMS measurement. A general description of how to incorporate diffraction into EMS has been formulated,⁵ but actual implementation is not straightforward, especially for our spectrometer that detects a range of outgoing trajectories simultaneously⁶ with varying diffraction conditions. Inclusion of inelastic energy loss processes in these calculations, although possible in principle, would make them even more involved.

In practice, MC simulations turned out to be more insightful⁷ and these simulations reproduced the effects of

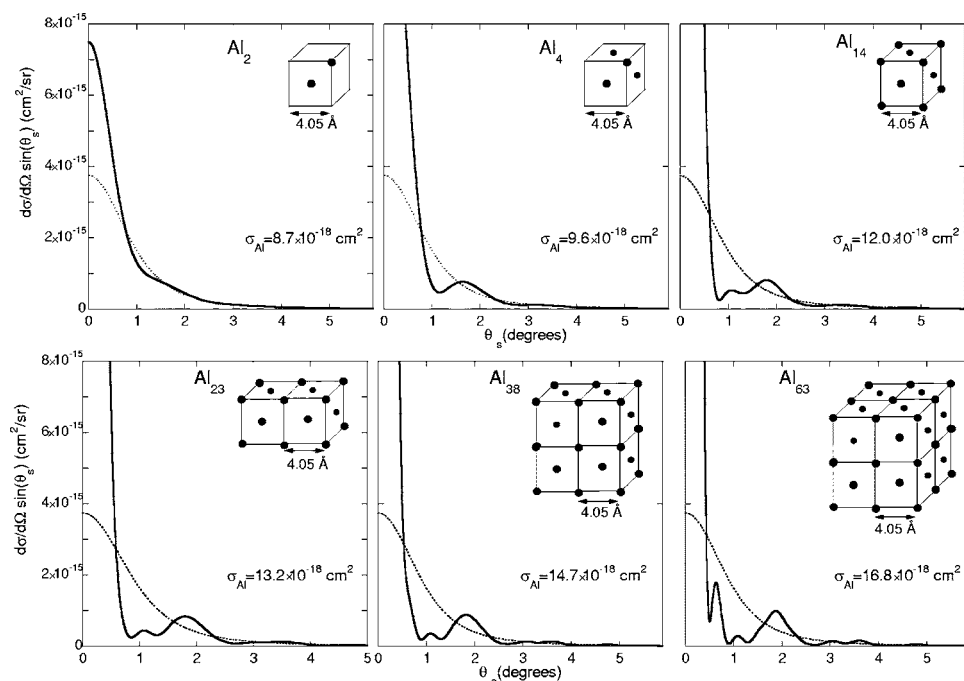


FIG. 1. Differential elastic cross section (normalized per aluminum atom) for 25 keV electrons scattering from different Al clusters as indicated, compared to the differential elastic cross section of an isolated Al atom (dashed line).

multiple scattering on momentum distributions obtained by EMS for amorphous and polycrystalline samples qualitatively, but perfect agreement was not obtained.^{8,9} Here we present a procedure that incorporates diffraction effects into the MC simulations for polycrystalline samples. A much improved description of the measured momentum distributions is obtained. We expect this procedure to be of use for a larger class of problems, dealing with small-angle deflections of electrons as well as their energy-loss processes.

In MC models of elastic scattering the wave nature of electrons is only considered in the derivation of the elastic scattering cross sections. As the deflections happen close to the nuclei, where the field seen by the electron is not affected significantly by solid-state effects, one uses atomic differential scattering cross sections as derived from fully quantum-mechanical calculations (e.g., Born approximation at very high energies, or partial wave analysis). The results of these calculations are used as input in the MC simulations which assumes particle trajectories rather than waves, and the simulations derive the average separation of elastic scattering events from the total elastic cross section and the magnitude of the deflection from the shape of the differential cross section as described in detail by, e.g., Shimizu and Ding.¹

In diffraction calculations, the propagation of electrons through the sample is described by interfering waves. Energy loss processes are usually neglected or dealt with in a simplified way (absorption). For polycrystalline samples the result is the average of many single-crystal calculations.

In this paper we choose an intermediate approach. We calculate the cross section not of an individual atom, but for a cluster of atoms. Rather small clusters reproduce the main diffraction features semiquantitatively. The differential cross section of the cluster is averaged over all its possible orientations. This cross section differs from the single-atom cross

section for small scattering angles, as the phase relation of waves emanating from different atoms in the cluster is taken into account. Subsequently a MC simulation is performed using the cluster cross section as input.

The differential cross section calculations were done using the ELSCATM program of the ELSEPA package from Salvat *et al.*¹⁰ It calculates the elastic scattering cross section of molecules, averaged over all possible orientations. Here we consider these molecules to be aluminum clusters. The structure of the clusters is identical to the arrangement of atoms in an Al crystal. The obtained differential cross sections (divided by the number of atoms of the cluster) are shown in Fig. 1.

In spite of this normalization, the differential cross section at zero degrees increases proportionally to the number of atoms in the cluster N_{cl} . This is expected since the waves emanating from all atoms are in phase at zero degrees, and the intensity will thus be proportional to N_{cl}^2 . The width of this peak is proportional to $1/\sqrt[3]{N_{cl}}$. At larger angles, the differential cross section of the cluster is less than that of an isolated atom, since the contribution of different atoms is out of phase for most molecular orientations. Pronounced peaks develop in the differential cross section at specific angles, becoming sharper with increasing cluster sizes. These are the equivalent of the diffraction rings observed in diffraction experiments of polycrystalline samples. The correspondence is obvious in Fig. 2, where we compare the cross section of a cluster of 63 Al atoms (for an energy of 50 keV) with the experimentally observed diffraction intensity as obtained from a phosphor screen in our spectrometer as well as the intensity for polycrystalline Al as predicted by the kinematic theory of diffraction.¹¹ The observed peaks are narrower than the calculated peaks, indicating that larger clusters are necessary to produce perfect agreement. Both positions and in-

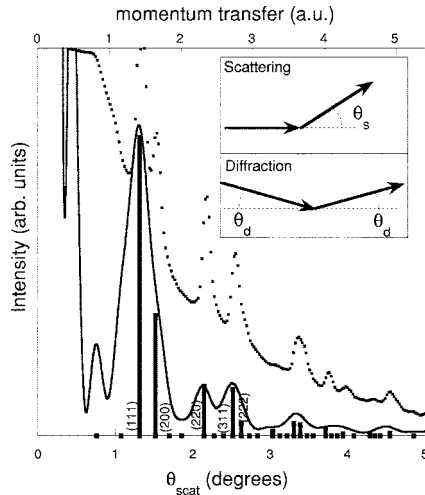


FIG. 2. Measured diffraction intensity (points) for a 50 keV electron and the scattering cross section for a 63 atom Al cluster (solid line), as well as the intensity calculated for polycrystalline Al using kinematic diffraction theory (vertical bars). The inset shows the difference in the definition of θ in the scattering and diffraction literature.

tensities match surprisingly well. The experimental peaks are, however, on a much larger background, attributed, at least in part, to electrons that also have scattered inelastically.

The total elastic cross section is given by

$$\sigma_{el} = \int_0^\pi \frac{d\sigma}{d\Omega} 2\pi \sin(\theta) d\theta. \quad (4)$$

Somewhat surprisingly, the calculated total elastic cross section per Al atom (σ_{al}) increases with cluster size, as indicated in Fig. 1 (elastic cross section of a single Al atom is $8.19 \times 10^{-18} \text{ cm}^2$ at 25 keV). Hence it follows from Eq. (1) that the calculated elastic mean free path λ_{el} decreases with assumed cluster size.

In Fig. 3 (upper panel) we show the differential cross section over a much larger angular range. Clearly the increase in the total cross section with increasing cluster size is due to its behavior at small angles. Thus with increasing cluster size more and more of the collisions will correspond to extremely small deflections. If these deflections are smaller than the experimental resolution then they will not affect the measurement. However, this limit is obtained for very large cluster sizes $N_{cl} \approx 1000$, and λ_{el} becomes impractically small.

Unfortunately, even after weighting the differential cross section by $\sin(\theta)$ [Fig. 3 (lower panel)], it is clear that for a cluster size of 63 atoms the forward peak is much wider than the momentum resolution of the experiment (0.1 a.u. corresponding to $\theta_s = 0.13^\circ$ at 25 keV), and hence simulations, including the large forward peak, would cause artificial broadening. Hence we decided to eliminate this artifact of the model in the following somewhat *ad hoc* way. We assume that the total elastic cross section is independent of cluster size. We calculate the lower boundary θ_0 such that

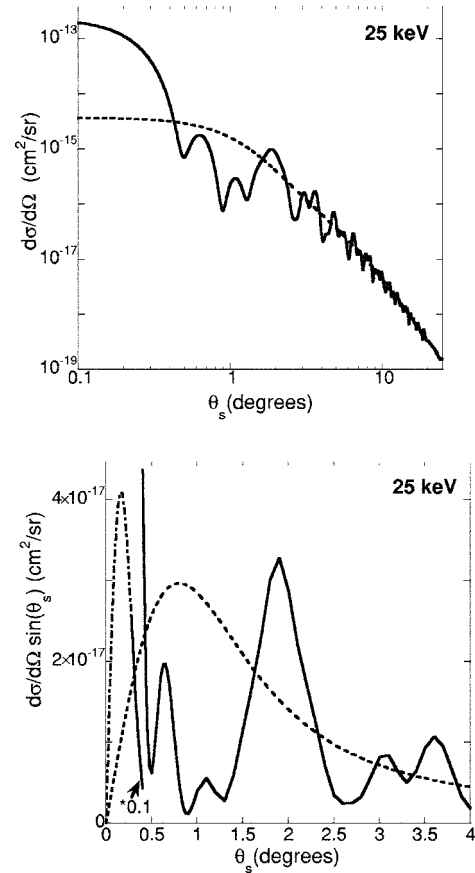


FIG. 3. A comparison of the cluster cross section (full line) and the single atom cross section (dashed) for the Al_{63} cluster over a large angular range (upper) and the magnitude of the cross section weighted by $\sin(\theta)$ (lower panel). The part shown as a dashed-dotted line is set to zero in the simulation.

$$\int_{\theta_0}^\pi \frac{d\sigma}{d\Omega} 2\pi \sin(\theta) d\theta = \sigma_1 \quad (5)$$

with σ_1 the cross section of a single Al atom. $\theta_0 = 0.26^\circ$ at 25 keV and $\theta_0 = 0.18^\circ$ at 50 keV. The differential cross section is set to zero for scattering angle $\theta_s < \theta_0$.

We will now show that EMS spectra of aluminum can be described much better with cluster cross sections than with atomic cross sections. Details of the experiment are given elsewhere.^{8,9} The electronic structure of Al approximates closely a free electron gas. Near the Fermi level only states with $q = k_f$ are occupied, with $k_f = 0.93 \text{ a.u.}$, the Fermi vector for aluminum. Our spectrometer is constructed in such a way that, without multiple scattering, only target electrons with $q_x \approx 0$, $q_z \approx 0$ can cause a coincidence. Using Eq. (2) we can select events that originate from electrons near the Fermi level. Without multiple scattering we expect to observe two peaks at $q_y = \pm k_f$. This is indeed the case (see Fig. 4), except for a background. This background is attributed to elastic multiple scattering, i.e., small deflections of the incoming and/or the outgoing electrons. If the total momentum transfer due to these small angle deflections is \mathbf{p} , then the Fermi sphere of Al appears shifted by this value. For these events,

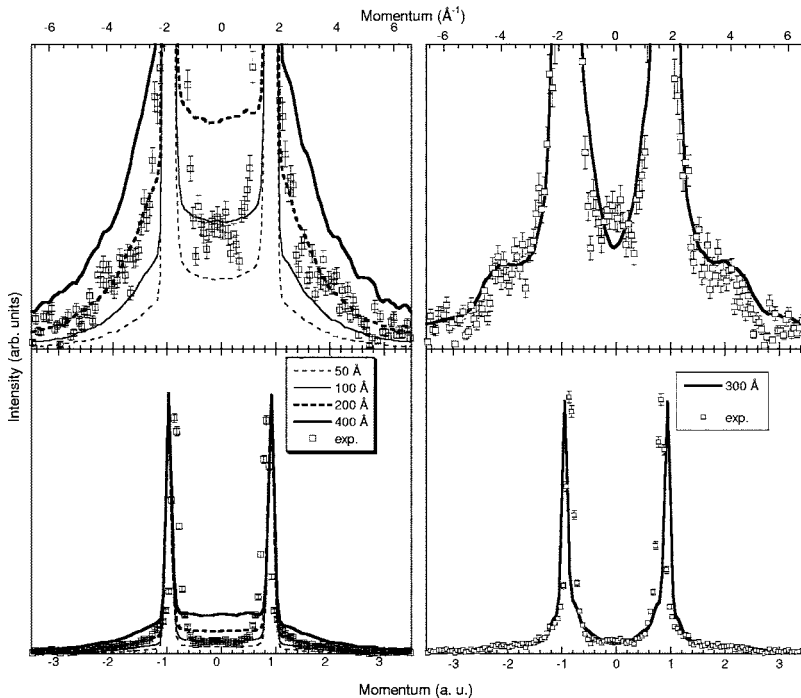


FIG. 4. A comparison of the results of MC simulations using atomic cross sections (left) and cluster-derived cross sections (right). In order to improve the statistics, the experimental and simulated results are integrated over binding energies between 0 and 2.5 eV. The top panels show the same data on a ten times expanded vertical scale.

intensity is expected at the intersection of the shifted Fermi sphere with the q_y axis.⁷

Since inelastic multiple scattering can only move intensity from the Fermi level to larger binding energy, inelastic scattering does not affect the shape of the observed momentum distribution at the Fermi level (but it reduces the overall intensity). Hence if we only compare the shape of the momentum density near the Fermi level, we are not affected by how well we treat inelastic multiple scattering; we see only the effects of elastic multiple scattering. Further details on the simulation approach are described in an earlier work.⁷

In the left panel of Fig. 4 we show the results of simulations using the elastic scattering cross section of an isolated atom as calculated by ELSEPA. We use the film thickness as a fitting parameter. These simulations show that elastic multiple scattering causes a background under the peaks, but fail, for any thickness, to describe the observed momentum profiles. If the simulated background is of the right magnitude at zero momentum, then it is much too small for large momentum values.

In the right panel we show simulations for a 300-Å-thick film, using the 63-atom-cluster cross section. The agreement between experiment and simulations has greatly improved compared to the “isolated atom” simulation. Even the shoulder at $|k_f|=2.2$ a.u. seen in the experiment is faithfully reproduced.

There is a clear physical interpretation why the isolated-atom derived cross section overestimates the multiple scattering contribution at $\mathbf{q}=0$. The smallest diffraction vector $\langle 111 \rangle$ corresponds to a momentum transfer of ≈ 1.5 a.u. (see Fig. 2). The Fermi sphere has a radius of 0.93 a.u. Intensity at zero momentum is then observed if $|p|=0.93$ a.u. The cross section is strongly reduced in the cluster calculation for angles corresponding to these momentum values.

We have shown that it is possible to incorporate diffraction effects in an approximate way in MC simulations of electron transport. This extends the applicability of MC simulations to situations where small-angle deflections influence the outcome of the experiment significantly. There is one implicit assumption in the simulation. If two subsequent deflections are within the same crystallite there will then be correlations between these deflections not contained in the simulations. Due to the small film thicknesses considered here, the length of the trajectories are on the average less than one mean free path long, hence double scattering in a crystallite will be a rather infrequent event in the current application.

The authors want to thank Les Allen and Erich Weigold for stimulating discussions. This work was made possible by a grant from the Australian Research Council.

¹R. Shimizu and Z.-J. Ding, Rep. Prog. Phys. **55**, 487 (1992).

²W. Werner, Surf. Interface Anal. **31**, 141 (2001).

³W. Smekal *et al.*, J. Electron Spectrosc. Relat. Phenom. **137**, 183 (2004).

⁴D. Liljequist, Nucl. Instrum. Methods Phys. Res. B **227**, 499 (2005).

⁵L. J. Allen *et al.*, Aust. J. Phys. **43**, 453 (1990).

⁶M. Vos, G. P. Cornish, and E. Weigold, Rev. Sci. Instrum. **71**,

3831 (2000).

⁷M. Vos and M. Bottema, Phys. Rev. B **54**, 5946 (1996).

⁸M. Vos, A. S. Kheifets, and E. Weigold, J. Phys. Chem. Solids **62**, 2215 (2001).

⁹M. Vos *et al.*, Phys. Rev. B **66**, 155414 (2002).

¹⁰F. Salvat, A. Jablonski, and C. J. Powell, Comput. Phys. Commun. **165**, 157 (2005).

¹¹J. Lábár, Microscopy and Analysis **75**, 9 (2002).